STAP moving target position estimation accuracy improvement and false detection recognition using a priori road information

André B. C. da Silva, Stefan V. Baumgartner

Microwaves and Radar Institute, German Aerospace Center (DLR)
Muenchener Str. 20, Oberpfaffenhofen, Germany
email: andre.silva@dlr.de

Abstract: *We have recently presented a processor for traffic monitoring applications that combines the post-Doppler space-time adaptive processing (PD STAP) with a road map obtained from the freely available OpenStreetMap (OSM). In this paper, the positioning error model of this processor is presented and discussed. In fact, two error models are combined: one for the PD STAP detections and one for the OSM road points. The positioning error model is essential for obtaining robust and reliable results. It was tested using real 4-channel aperture switching radar data acquired by the DLR's airborne system F-SAR. The results reveal a powerful algorithm that recognizes and rejects most of the false detections, being suitable for many traffic monitoring applications.*

1. Introduction

The number of road vehicles is increasing worldwide, leading to congestions. The methods employed nowadays for monitoring and counting the vehicles on the roads are expensive and limited in spatial coverage (e.g., cameras, induction loops, or even people manually counting). Synthetic aperture radars (SAR) provide an effective solution for this problem due to the wide-area coverage and the independence from daylight and weather conditions [1-2]. Special attention is given in case of large scale events or catastrophes, when mobile internet is unavailable and phone communication is impossible. In this particular scenario, the traffic monitoring with real-time information ensures the safety of the road users and can even save lives.

Several solutions are found in the literature for traffic monitoring using SAR. For instance, the algorithm presented in [3] combines the powerful post-Doppler space-time adaptive processing (PD STAP) with a road map from the freely available OpenStreetMap (OSM). The incorporation of a known road network into the processing chain presents great potential for real-time processing, since only the acquired data related to the roads need to be processed. As a result, decreased processing hardware complexity and low costs compared to state-of-the-art systems can be achieved. In addition, it is a promising solution for detecting effectively the road vehicles and estimating their positions, velocities and moving directions with high accuracy. A follow-up version of this algorithm is presented in [4], where a PD STAP's performance model is employed for providing an adaptive relocation threshold – used to decide if the target is actually a road vehicle or a false detection. Nevertheless, it is pointed out that additional errors should still be considered, i.e., a positioning error model is needed.

This paper presents a positioning error model for increasing the robustness and the reliability of our PD STAP processor. In brief, a position error model is derived for the OSM road points and combined with the position error model for STAP presented in [5]. As a result, most of the false detections can be recognized and rejected.

2. Signal Processing Algorithm

The simplified flowchart of our PD STAP processor is shown in Fig. 1. An *Initial Procedure* is carried out in order to estimate (mainly): the covariance matrix (required by the PD STAP for clutter suppression), the antenna pattern and the baselines. Note that this procedure needs to be updated regularly, since the estimated covariance matrix must always match the data.

The processor operates directly on multichannel range-compressed (RC) data. The *Calibration* step is applied for correcting the residual along-track interferometry (ATI) phase and the data amplitude. Optionally, the data Doppler centroid can also be shifted to zero. The PD STAP is well-known in the literature [6-9] and is used for estimating the line-of-sight velocity, the Doppler frequency and the direction-of-arrival (DOA) angle of the target. In the *Coordinate Transformation* block, the detections (in radar coordinates) are converted into the Universal Transverse Mercator (UTM) coordinate system.

The *Post-Detection Module* is presented in detail in [3,4] and includes two databases: the OSM and a digital elevation model (DEM). Note that the DEM is necessary because the OSM does not provide height information. For each coherent processing interval (CPI), the roads of interest are selected and an interpolation is carried out to fill possible gaps between the road points. The OSM provides the angle and the position of each road point. The road point angle allows the computation of the absolute velocity of the target on the road, using the slant-range velocity of the target estimated by the PD STAP. The Performance Model requires the signal-to-clutter plus noise ratio (SCNR) and the slant-range velocity of the target for estimating the accuracy of the target azimuth angle (Cramér-Rao bounds). This parameter is used by the PD STAP position error model [4,5].

The *Error Models & Decision* block includes two position error models: one for PD STAP and one for OSM (see Section 3). By applying both error models, a decision can be made if the target is a vehicle moving on the road or a false detection. If the first case is true, the target is repositioned to the nearest road point; otherwise it is discarded as a false detection (which is also the case for cars moving off-road).

At the end of the processing chain, the data are formatted (e.g., Keyhole Markup Language (KML) files can be generated for visualization in Google Earth) and finally distributed (e.g., to the traffic management center).

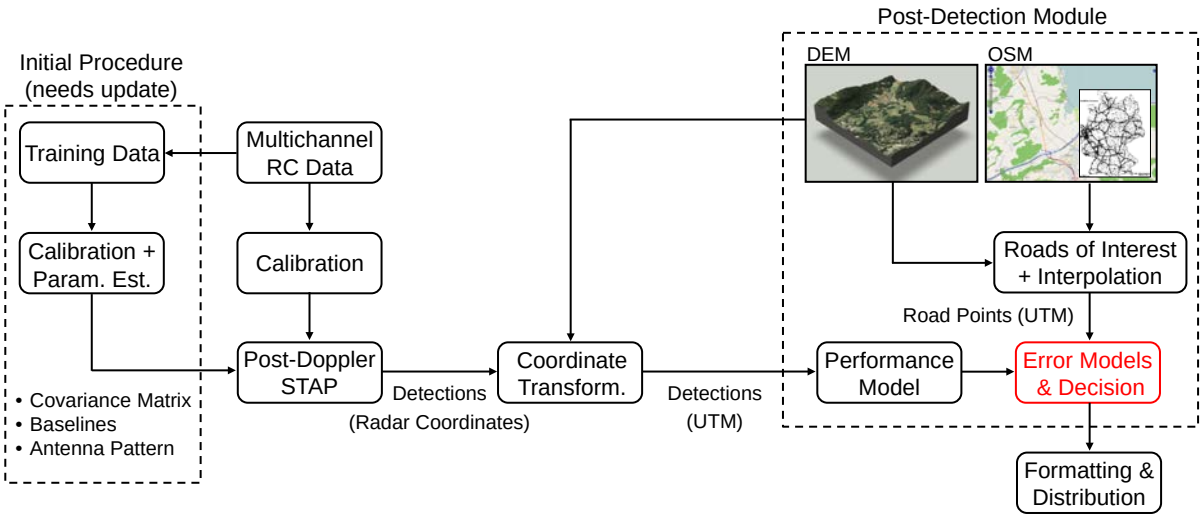

Figure 1. Simplified flowchart of the PD STAP processor. The *Error Models & Decision* block is presented and discussed in this paper.

3. Error Models and Decision

This section describes the positioning error models for the PD STAP detections and for the OSM road points. At the end, two error ellipses are obtained (i.e., one for each error model), as shown in Fig. 2. In this figure, r_{10} is the slant range of the target, α_p is the flight course of the platform measured with respect to the UTM easting axis, and $\theta_{t,x}$ is the DOA angle of the target projected on ground and measured with respect to the azimuth direction. As a first approach, the detection is a road vehicle if an overlapped area exists between both ellipses.

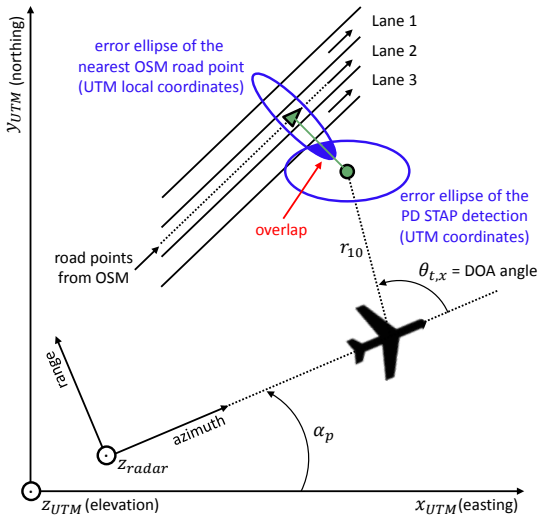

Figure 2. Geometry showing the error ellipses of the PD STAP detection and its nearest OSM road point.

3.1. Error Model for STAP

The positioning error model for the PD STAP detections uses the framework presented in [5], whereas the position accuracy of the target is calculated by error propagation using the variance formula, expressed generally as:

$$\sigma_y = \sqrt{\sum_{i=1}^{m} \left(\frac{\partial_y}{\partial_{x_i}} \right)^2 \sigma_{x_i}^2}\ ,\ y = f(x_1,\ldots,x_n), \tag{1}$$

where σ_y is the standard deviation and $(x_1,\ldots,x_n)$ is a collection of independent random variables. The positioning errors are obtained in the UTM coordinate system.

3.2. Error Model for OSM

The positioning error model for the OSM road points is presented according to the geometry shown in Fig. 3, in local UTM coordinates, for the particular case of a road with five lanes. This figure shows that only one road axis is provided by the OSM database, normally at the center of the road (e.g., lane 3). In this sense, let (x_{osm}, y_{osm}, z_{osm}) be the true UTM coordinates of a road vehicle moving in a particular lane (e.g., lane 5), and let (x'_{osm}, y'_{osm}, z'_{osm}) be the UTM coordinates of the road axis (i.e., the OSM road points). In practice, the lane of the road vehicle is not known, and thus a position error $\delta_{y_{osm}}$ has to be considered in the error model.

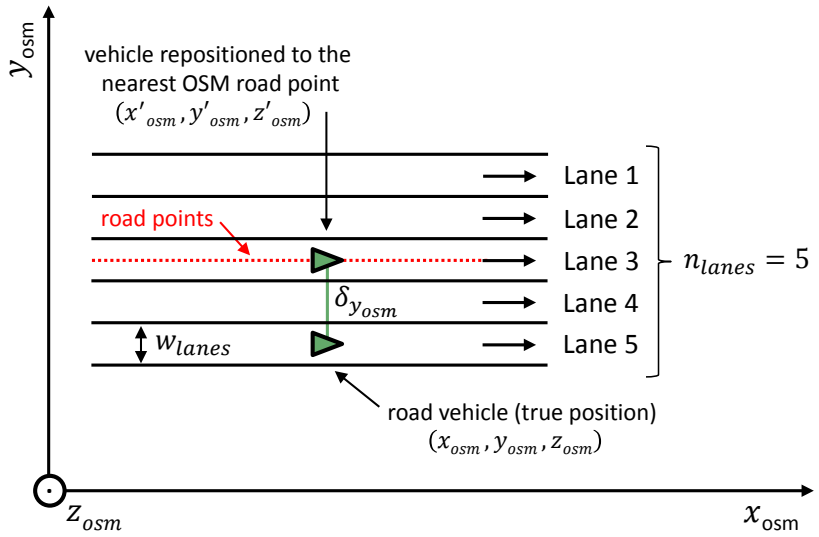

Figure 3. Geometry of the OSM road points' positioning error: example of a road with five lanes in local UTM coordinates. An error is observed due to the distance between the road axis and the lane of the road vehicle.

By assuming a sufficiently small interpolation distance between the OSM road points, and that the road vehicle moves at the center of its lane, we have that:

$$x_{osm} = x'_{osm} \ , \tag{2}$$

$$y_{osm} = y'_{osm} - \delta_{y_{osm}} \ , \tag{3}$$

$$\delta_{y_{osm}} = \frac{w_{lanes}\left(n_{lanes} - 1\right)}{2} \ , \tag{4}$$

where n_{lanes} is the number of lanes of the road and w_{lanes} is the width of each lane. Thus, the position accuracy of the OSM road points can be calculated by error propagation using the variance formula:

$$\sigma_{x_{osm}} = \sqrt{\left(\frac{\partial_{x_{osm}}}{\partial_{x'_{osm}}}\right)^2 \sigma^2_{x'_{osm}}} \ , \tag{5}$$

$$\sigma_{y_{osm}} = \sqrt{\left(\frac{\partial_{y_{osm}}}{\partial_{y'_{osm}}}\right)^2 \sigma^2_{y'_{osm}} + \left(\frac{\partial_{y_{osm}}}{\partial_{n_{lanes}}}\right)^2 \sigma^2_{n_{lanes}} + \left(\frac{\partial_{y_{osm}}}{\partial_{w_{lanes}}}\right)^2 \sigma^2_{w_{lanes}}} \ . \tag{6}$$

Since independent random variables are assumed, the calculation of the derivatives results in:

$$\sigma_{x_{osm}} = \sigma_{x'_{osm}} \ , \tag{7}$$

$$\sigma_{y_{osm}} = \sqrt{\sigma^2_{y'_{osm}} + \frac{w^2_{lanes}}{4}\sigma^2_{n_{lanes}} + \left(\frac{n_{lanes} - 1}{2}\right)^2 \sigma^2_{w_{lanes}}} \ . \tag{8}$$

4. Experimental Data

The positioning error model was tested using real 4-channel aperture switching data acquired by the DLR's airborne system F-SAR. The flight campaign was conducted in February 2007 over the Allgäu airport in Memmingen, where five controlled cars were considered. The cars' velocities and the radar parameters are given in [10]. The data were processed using data blocks of 1024x128 range-Doppler samples, and the beamformers were applied using DOA angle steps of 0.1° within an interval determined by the azimuth antenna beam width [3,4].
The experimental results are shown in Fig. 4, where the radar detections are shown as a Google Earth overlay and the center of the runway (yellow line) was considered as the road axis. The detections are shown before (circles) and after (triangles) the reposition using the road map, where the colors are related to the velocities of the cars and the triangles point to their moving direction. The white ellipses show the position error of the PD STAP detections, and the blue ellipses show the position error of the detections' nearest road points.
The parameters used in the positioning error models are shown in Table 1. It is pointed out that the number and the width of the road lanes (as well as their standard deviations) were calculated taking into account roads in different regions of Germany.
The result shown in Fig. 4 is a special case, since the width of the runway is much larger than a normal road, and besides, the vehicles moved on the edges of the lanes. For that reason, the width of the road lanes in this case was set to 15 m. The estimated accuracy of the target azimuth angle was $\sigma_{\theta_{t,x}}$ = [0.005° to 0.659°].

Fig. 5 shows a real traffic scenario in the Memmingen area with a large number of vehicles of opportunity (detail: car moving in the highway A7). The parameters from Table 1 were used, and the estimated accuracy of the target azimuth angle was $\sigma_{\theta_{t,x}}$ = [0.010° to 0.592°].

Table 1. Parameters of the positioning error models.

Position accuracy of the platform (GPS/DGPS)	$\sigma_{x_p} = \sigma_{y_p} = \sigma_{z_p}$ = 0.29 m
Accuracy of the height of the scene (e.g., the DEM's accuracy)	σ_{z_t} = 10 m
Accuracy of the target slant-range	$\sigma_{r_{10}}$ = 1.2 m
Accuracy of the flight course (after motion compensation)	σ_{α_p} = 0.03°
Accuracy of the OSM position	$\sigma_{x'_{osm}} = \sigma_{y'_{osm}}$ = 3 m
Accuracy of the number of road lanes	$\sigma_{n_{lanes}}$ = 0.86
Accuracy of the width of the road lanes	$\sigma_{w_{lanes}}$ = 0.40
Number of road lanes	n_{lanes} = 2.72
Width of the road lanes	w_{lanes} = 3.40

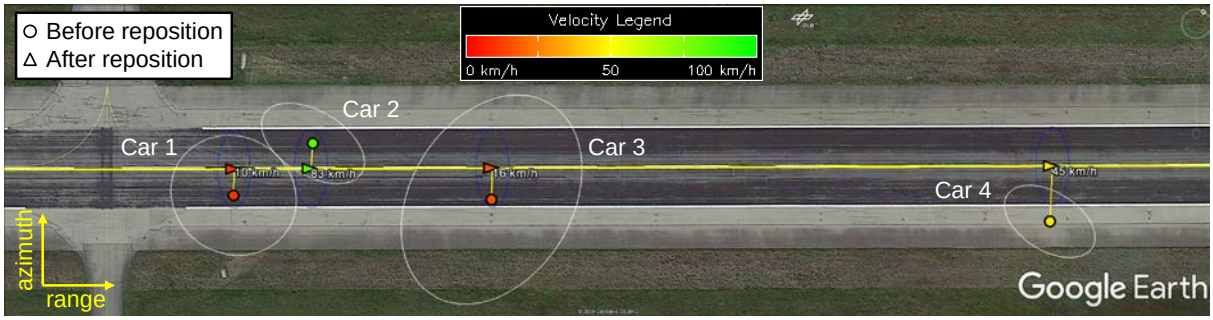

Figure 4. Runway of the Allgäu airport in Memmingen (image size: 140 x 440 m): Google Earth image overlaid with radar detections before (circles) and after (triangles) reposition. The ellipses show the positioning error of the PD STAP detections (white) and their nearest OSM road points (blue). The road axis is shown in yellow.

Figure 5. Real traffic scenario in the Memmingen area (image size: 1.0 x 1.8 km). The considered OSM road axes are shown in yellow and the velocities of the cars (triangles) are printed and color coded according to the legend. The cars were detected and their parameters were automatically estimated using our PD STAP processor.

For the results presented in this section, a clustering algorithm was applied in order to select the peak detection of each vehicle inside each CPI. Moreover, an error of $\pm 2\sigma$ was assumed (i.e., $\approx$ 95% confidence level). As a matter of fact, the confidence level influences directly on the sizes of the error ellipses, and therefore, also on the number of detections.

The most sensitive parameters of the STAP error model are: the accuracy of the target azimuth angle and the accuracy of the height of the scene. In the first case, it is pointed out that slower vehicles present a lower SCNR, which lead to a higher azimuth relocation error, as shown in [4]. The second case highlights the importance of having the DEM in the processing chain in order to reduce the positioning error. In contrast, the position accuracy of the platform has a minor impact in the error model, and besides, it is normally known.

In Fig. 5, since no ground truth data were available, it is not possible to determine the probability of detection, the false alarm rate and the errors of the estimated parameters. Nevertheless, the estimated velocities on the highway A7 and on the residential roads seem reasonable.

5. Conclusion

The positioning error model used in our PD STAP processor was tested using real 4-channel aperture switching data acquired by the DLR's airborne system F-SAR. The experimental results revealed a robust and reliable algorithm that can recognize and reject most of the false detections, being suitable for many traffic monitoring applications.

References

[1] A. Moreira, et al.: A tutorial on synthetic aperture radar, IEEE Geosci. Remote Sensing Mag., vol. 1, no. 1, pp. 6-43, 2013.

[2] K. Tomiyasu: Tutorial review of synthetic-aperture radar (SAR) with applications to imaging of the ocean surface, Proceedings of the IEEE, vol. 66, no. 5, pp. 563-583, May 1978.

[3] A. B. C. da Silva and S. V. Baumgartner: A priori knowledge-based STAP for traffic monitoring applications: first results, in Proc. EUSAR, Hamburg, Germany, Jun. 2016.

[4] A. B. C. da Silva and S. V. Baumgartner: Novel post-Doppler STAP with a priori knowledge information for traffic monitoring applications, in Proc. Kleinheubacher Tagung, Miltenberg, Germany, Sep. 2016.

[5] D. Cerutti-Maori, et al.: Wide-area traffic monitoring with the SAR/GMTI system PAMIR, IEEE Trans. on Geoscience and Remote Sensing, vol. 46, no. 10, pp. 3019-3030, 2008.

[6] W. L. Melvin: A STAP overview, Aerospace and Electronic Systems Magazine, IEEE, vol. 19, no. 1, pp. 19-35, Jan. 2004.

[7] J. H. G. Ender: Space-time processing for multichannel synthetic aperture radar, Electr. and Comm. Eng. J., pp. 29-38, 1999.

[8] J. R. Guerci: Space-time adaptive processing for radar, Artech House. 2014.

[9] R. Klemm: Space-time adaptive processing, The Institute of Electrical Engineers, London, United Kingdom, 1998.

[10] S. V. Baumgartner and G. Krieger: Fast GMTI algorithm for traffic monitoring based on a priori knowledge, IEEE Trans. on Geoscience and Remote Sensing, vol. 50, no. 11, pp. 4626-4641, 2012.